Synchronous generator damping enhancement through coordinated control of exciter and SVC

A.H.M.A. Rahim
S.G.A. Nassimi

Indexing terms: Power system stability, SVC, Excitation control

Abstract: Damping improvement of a weakly connected generating system through control of excitation and static VAr compensators has been investigated. Stabilising signals derived through a minimum time quasioptimum feedback strategy have been tested on a synchronous generator infinite bus system connected through a long transmission line. The response was compared with standard linear state and output regulator formulations. It was observed that although excitation control enhances the stability of the system, the SVC provides most of the damping. The proposed feedback strategy with coordinated control of excitation and SVC were found to provide a much superior response compared to the standard techniques.

1 Introduction

Transient stability of synchronous generators located far from the major load centres are improved by the introduction of static excitation systems. This, however, deteriorates synchronous generator damping. Power system stabilisers (PSS) have been a matter of intensive study and most modern power systems are equipped with these devices. While excitation controllers are normally effective in damping power oscillations, they suffer a drawback of being liable to cause a great variation in the voltage profile and they may even result in leading power factor operation under severe disturbance conditions [1].

Thyristor-controlled reactors and capacitors, termed as static VAr compensators (SVC) are well known to improve power system properties such as steady-state stability limits, voltage regulation and VAr compensation, dynamic over-voltage and under-voltage control, counteracting subsynchronous resonance, and damp power oscillations [2, 3]. Voltage controlled SVC, as such, does not provide any damping [4, 5]. However, additional signals through SVC voltage control loop has been observed to provide extra damping [4, 6, 7].

IEE Proceedings online no. 19960194

Paper first received 19th April 1995 and in revised form 17th November 1995

A.H.M.A. Rahim is with the Department of Electrical Engineering, K.F. University of Petroleum and Minerals, Dhahran, Saudi Arabia

S.G.A. Nassimi is with the Department of Electrical Engineering, University of Bahrain, Isa Town, Bahrain

Control functions similar to those in the PSS are used to generate a signal for the voltage control loop and various signals like power, frequency, etc. are used as input to the control function. An alternative suggested is to provide a stabilising signal at the output of the voltage control loop to control the firing angle of the thyristors [8]. The signals could be continuous or discontinuous. Bang-bang control of system susceptance through appropriate firing angle control has been demonstrated to provide very good damping [3, 5, 9]. Reference [3] proposes optimum bang-bang control of susceptance to the extreme available limits depending on iteratively obtained costate variables, while [5, 9] propose discontinuous controls on the basis of transmission line power or power angle variations in the system.

Many of the systems for which SVC usage has been considered involve transmission over long distances from remote sources of generation. Such systems tend to be poorly damped, and their high series impedance means that controls on alternator exciters may be relatively ineffective [10]. Since most of these generators may have been equipped with excitation controls, for any control action on the SVC to damp the system oscillations, the controls must be properly coordinated. Though there is vast amount of material available in the literature on individual control of excitation and SVC, research on coordinated application of these controls, particularly application of optimal control, is generally limited. A recent study on coordinated excitation and SVC control through the reduced-order model obtained by estimation techniques indicates that damping can be effectively increased by both measures [1]. However, a comparative analysis of the controls was lacking and their relative merits are not obvious. Also, linear quadratic controls are operating condition-dependent and, hence, are limited in terms of application.

In this article, a systematic study of the effects of excitation and SVC control when applied independently and also through coordinated application has been carried out. Comparison of the two controls has been made using the linear state and output regulator formulations. Optimum feedback strategies for both SVC and exciter controls have been proposed and the results are compared with the regulator strategies. The various control strategies have been tested on a single generator infinite bus system. It was observed that proposed coordinated optimum feedback control provides very good damping.

2 Linear dynamic model of single machine system

The power system configuration shown in Fig. 1 is considered for this study. The generator is located at a remote point from the load centre which is represented by the power system bus in the figure. The SVC is placed at the middle of the transmission line which has been reported to be the ideal site [5, 11]. The generator has a local load represented by the admittance $Y_L = g - jb$, and it is assumed to be equipped with a static excitation system. The governor dynamics is ignored in the analysis. The generator is represented by a third-order model comprising of the electromechanical swing equation and the generator internal voltage equations. The electromechanical swing equation is broken up into

$$p\delta = \Delta\omega \quad (1)$$

$$p\Delta\omega = (P_m - P_e - D\Delta\omega)/M \quad (2)$$

where, P_m and P_e are the input and output powers of the generator, respectively; M and D are the inertia constants and damping coefficients; δ and ω are the rotor angular positions and angular frequency; p is the derivative operator d/dt. The power output of the generator expressed in terms of direct (d) and quadrature (q) axes components of voltage (v) and current (i) is

$$P_e = v_d i_d + v_q i_q \quad (3)$$

The internal voltage equation is

$$\Delta e_q' = [e_{fd} - (x_d - x_d')i_d]/(1 + pT_{do}') \quad (4)$$

Here, e_{fd} is the generator field voltage and T_{do}' is the open circuit field time constant. The exciter and voltage regulator is represented by the block diagram shown in Fig. 2. The differential equation relating the field and terminal voltage is written as

$$p\Delta e_{fd} = K_A[v_{tr} - v_t + u_s]/T_A - \Delta e_{fd}/T_A \quad (5)$$

Here, the terminal voltage v_t is expressed through

$$v_t^2 = v_d^2 + v_q^2 \quad (6)$$

where v_{tr} is the reference voltage setting and u_s is the additional control signal. The d,q components of armature current and termimal voltage i_d, i_q, v_d and v_q, respectively, are obtained from the algebraic equations relating the transmission line quantities and the generator internal voltage relationship as [12]

$$\begin{bmatrix} v_d \\ v_q \end{bmatrix} = \begin{bmatrix} 0 \\ 1 \end{bmatrix} e_q' - \begin{bmatrix} 0 & x_q \\ -x_d' & 0 \end{bmatrix} \begin{bmatrix} i_d \\ i_q \end{bmatrix}$$

$$\begin{bmatrix} i_d \\ i_q \end{bmatrix} = \begin{bmatrix} Y_d \\ Y_q \end{bmatrix} e_q' - \frac{v_o}{z_e^2} \begin{bmatrix} R_3 & X_2 \\ -X_3 & R_2 \end{bmatrix} \begin{bmatrix} \sin\delta \\ \cos\delta \end{bmatrix} \quad (7)$$

Note that Y_d, Y_q, R_2, R_3, etc. are functions of susceptance B.

Substituting the expressions for i_d, i_q, v_d and v_q in eqns. 3 and 4 and subsequently in eqn. 2, eqns. 1–5 can be expressed as

$$\dot{Y} = f(Y, B, u_s) \quad (8)$$

where, Y is a vector of the following variables: generator rotor angular position, frequency variation, internal voltage and field voltage. Linearising eqn. 7, the generator currents are expressed as

$$\begin{bmatrix} \Delta i_d \\ \Delta i_q \end{bmatrix} = \begin{bmatrix} E_{11} & E_{12} & E_{13} \\ E_{21} & E_{22} & E_{23} \end{bmatrix} \begin{bmatrix} \Delta\delta \\ \Delta e_q' \\ \Delta B \end{bmatrix} \quad (9)$$

which when substituted into the linear form of eqns. 1–5 yield the system equations

$$\dot{X} = AX + bu \quad (10)$$

Here, the state vector X is $(\Delta\delta, \Delta\omega, \Delta e_q', \Delta e_{fd})^T$ and the control vector u is $(\Delta B, u_s)^T$.

The outputs of the system are selected to be the voltage (v_m) and power (p_m) at the midpoint of the transmission line where the SVC is connected. The linearised form of the output equations, as given in Appendix A, are

$$\begin{bmatrix} \Delta v_m \\ \Delta p_m \end{bmatrix} = \begin{bmatrix} r_{11} & r_{12} \\ r_{21} & r_{22} \end{bmatrix} \begin{bmatrix} \Delta\delta \\ \Delta e_q' \end{bmatrix} + \begin{bmatrix} w_1 \\ w_2 \end{bmatrix} \Delta B \quad (11)$$

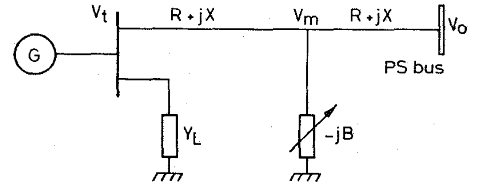

Fig. 1 *Power system configuration*

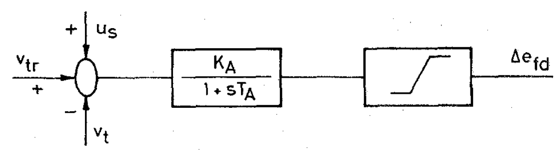

Fig. 2 *The static exciter and regulator system*

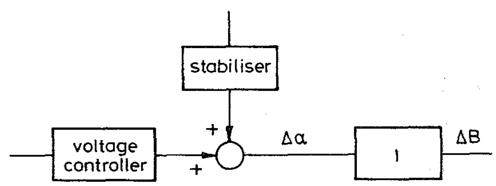

Fig. 3 *Susceptance control block diagram*

3 Stabilising control strategies for the linearised system

Two controls, one in the excitation system and the other in the SVC, are utilised to improve the system damping. The stabilising signal in the excitation system (u_s) is included in the AVR as shown in Fig. 2. The signal in the SVC is added at the output of the voltage control loop which controls the firing angle of the thyristors, thus changing the susceptance B of the SVC. This is illustrated by the block diagram given in Fig. 3.

Various optimal and suboptimal strategies for finding controls u_s and ΔB are presented here. Linear state and output regulator formulations are followed by the proposed feedback strategy for stabilisation.

3.1 The optimum linear state regulator control

The linear state regulator problem is well documented in the literature [12] and is restated here briefly. For the linear system, eqn. 10, the control $u^*(t)$ which minimises

$$J = \frac{1}{2}\int_{t_o}^{t_f} (X^T Q X + u^T R u)\, dt \quad (12)$$

is given by the feedback control law

$$u^* = -R^{-1}B^T K X(t) \quad (13)$$

where K is the solution of the matrix Riccati equation

$$0 = A^T K + KA - KBR^{-1}K^T + Q \quad (14)$$

The static Riccati equation given in eqn. 14 can be solved in a closed form.

3.2 The linear output regulator control

If not all the state variables are accessible or measurable but only

$$Y(t) = CX(t) \quad (15)$$

is observable, then one way of expressing the suboptimal control as a function of the output is [13]

$$u^o(t) = -F^o CX(t) = -F^o Y(t) \quad (16)$$

where,

$$F^o = F^* \Lambda C^T (C \Lambda C^T)^{-1}$$

Λ is obtained from the solution of the matrix Riccati equation

$$(A - BF^*)\Lambda + \Lambda(A - BF^*)^T + I = 0 \quad (17)$$

and F^* is the control gain matrix in eqn. 13 rewritten as

$$u^*(t) = -F^* X(t) \quad (18)$$

3.3 The proposed optimum feedback control strategy

The linear state and output regulator strategies are normally precomputed depending on particular operating conditions. Hence, on-line applicability of such controls are limited. For on-line applications, the control strategies should preferably be independent of points of operation, and the variables to be fed back should be accessible with relative ease. However, the optimum state regulator and suboptimum output regulator controls provide good bases for comparison of any other strategies.

When a power system is perturbed from its normal operating condition, often it is required to bring the states back to their normal range as quickly as possible. This is particularly true when the oscillations could lead to unacceptable or unstable conditions. The stabilisation problem then can be posed as an optimum control problem as: Find the admissible control $u(t)$, subject to the magnitude constraint on it (normalised) given by

$$|u_i(t)| \leq 1 \qquad i = 1, 2 \quad (19)$$

which transfers the system given by eqn. 10 to one of its equilibrium states represented by $\Delta\omega = 0$ and $p\Delta\omega = 0$ and at the same time minimises the transition time, or minimises the cost functional given by

$$J = \int_{t_o}^{t_f} \mathrm{d}t \quad (20)$$

Since determination of optimum control as a function of states and other measurable quantities for the problem stated above is generally not easy, the following procedure to find quasi-optimum controls is now proposed.

3.3.1 Strategy for ΔB: Reconstruct the electromechanical swing equation from the set of eqn. 10, which is

$$p^2\Delta\delta = a_{11}\Delta\delta + a_{13}\Delta e'_q + b_1 u_1 \quad (21)$$

Here, control u_1 is ΔB. The first two terms in the right hand side is state-dependent. So, the equation can be expressed as

$$p^2\Delta\delta = L_B(x) + b_1 u_1 \quad (22)$$

In the absence of the $L_B(x)$ term, the time-optimal contol for system eqn. 22 subject to the constraints of eqn. 19 can be readily obtained in terms of switching curves involving $\Delta\delta$ and its derivatives [12, 14]. A quasi-optimum minimum time control for eqn. 22 considering that $L_B(x)$ is sufficiently small compared to b_1, u_1, can be written as

$$u_1 = -\operatorname{sgn} \Sigma_B \quad (23)$$

where

$$\Sigma_B = \Delta\delta - \frac{(p\Delta\delta)^2}{2[L_B(x) + b_1 \cdot \operatorname{sgn}\{p\Delta\delta\}]}$$

Here we assume that $L_B(x)$ is sufficiently slow-changing to be considered constant over each integration step. The optimal SVC control u_1 which eliminates the transients in minimum time is of bang-bang nature, changing between the maximum and minimum limits. This agrees with the concept presented by Hamad [2]. The switch function here, however, depends on system states and no iterative procedure is involved.

While it is possible to switch the controls almost instantaneously with fast switching devices, a more practical control strategy given below makes the control proportional to the switching function

$$u_1 = K_B \Sigma_B \quad (24)$$

Here, a proper value of K_B can be chosen so that the control reaches the ceilings when the oscillations are large.

3.3.2 Strategy for excitation and SVC control: Since the electromechanical swing eqn. 21 does not contain the excitation control term explicitly, we differentiate both sides of this equation to get

$$p^2\Delta\omega = a_{11}p\Delta\delta + a_{13}p\Delta e'_q + b_1 p\Delta B \quad (25)$$

The optimal ΔB is either the maximum or the minimum value as shown in eqn. 23. So, $p\Delta B$ is zero everywhere except at the points where the control switches. Substituting the expressions for $p\Delta\delta$ and $p\Delta e_q'$ from eqn. 10, eqn. 25 is written as

$$p^2\Delta\omega + c\Delta\omega = L_E(x, u_1) + b_E(x)u_2 \quad (26)$$

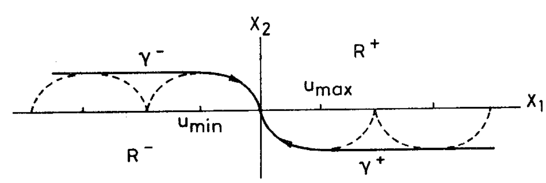

Fig. 4 *The switch curves for excitation control*

The term $c\Delta\omega$ is not included in $L_E(x, u_1)$ to make sure that it is reasonably small compared to the admissible values of $b_E(x)u_2$. A time-optimal control strategy, similar to the harmonic regulator problem [14], is illustrated by Fig. 4. The optimum switch curves are shown by the dashed semicirdes and the solid curves give a suboptimal strategy. The horizontal and vertical coordinates are $\Delta\omega$ and $\sqrt{cp\Delta\omega}$, respectively. The radii of the circles u_{max} and u_{min} are the maximum and minimum possible values of the right-hand side of eqn. 26. The term $b_e(x)$ is normally negative. If the states lie in R^+ i.e. on the right side of the switch curve $\gamma = \gamma_+ \cup \gamma_- = 0$, then control $u_2 = u_s$ is the maximum value. Similarly, u_s is a minimum when the states belong to R^-.

The excitation control switches when the trajectory hits γ. This can be written as

$$u_s = -\operatorname{sgn}\gamma \quad (27)$$

The time-optimal excitation control is also bang-bang in nature. The excitation can be forced to the ceilings by the additional control u_s in the voltage regulator. As in the SVC control, a more practical excitation control strategy is

$$u_s = K_E\gamma \quad (28)$$

This forces the excitation to the ceilings when the oscillations are large and lets normal AVR action take over when the transients have died down.

4 Extension to nonlinear and multimachine systems

The control strategy developed in the earlier section can be right away extended to the nonlinear model of a single machine system as well as to multimachine systems. For a multimachine power system, control design can be carried out globally considering the entire dynamics of the system or using the local controls. The latter takes the dynamics of each machine at a time including its interconnection to the rest of the network. In the following, we propose a scheme for local control of the SVC system for a multimachine system retaining the nonlinearities of the system model.

Consider the swing equation of the ith machine in the system (neglect damping), rewritten as

$$p^2\delta = (P_m - P_e)/M \quad (29)$$

The electrical power output of each machine from eqn. 3 is

$$P_e = v_d i_d + v_q i_q$$
$$= i_q e'_q + (x_q - x'_d) i_d i_q \quad (30)$$

Here, e_q', i_d and i_q are functions of susceptance B of each SVC controller, rotor angle δ of each machine with respect to the reference, and the bus voltage v_0 of the power network to which each generating system is connected. In the single machine modelling we considered v_0 to be constant but it is a variable quantity in the multimachine model.

Substituting eqn. 30 in eqn. 29, we can write

$$p^2\delta = f(e'_q, \delta, v_o, B)$$
$$= m(x) + n(x)u_1 \quad (31)$$

In the above, $m(x)$ includes all the terms independent of control $u_1(B)$ and $n(x)$ contains all the terms associated with control B.

Eqn. 31 is similar to eqn. 22 and hence the SVC control for the ith machine in the system can be expressed by an equation similar to eqn. 23, $L_B(x)$ replaced by $m(x)$ and b_1 replaced by $n(x)$, respectively. Eqn. 31 is derived considering the system nonlinearities and the control strategy does not depend on any specific operating condition. A strategy similar to eqn. 28 can be obtained for excitation control also.

5 Results

The single generator infinite bus system given in Fig. 1 was simulated for testing the effectiveness of the various controls presented. System data, the operating quantities and the system matrices for the linearised system are given in Appendix B. A number of disturbances were considered. The resulting response was studied with the following control signals:

(*a*) state regulator control

(*b*) output regulator control

(*c*) proposed minimum time feedback controls

In each case the response was recorded with SVC control and excitation control separately and also with coordinated application of both. The minimum time control of only the linearised system given in section 3 is considered because it can be readily compared with the linear state and output regulator control strategies.

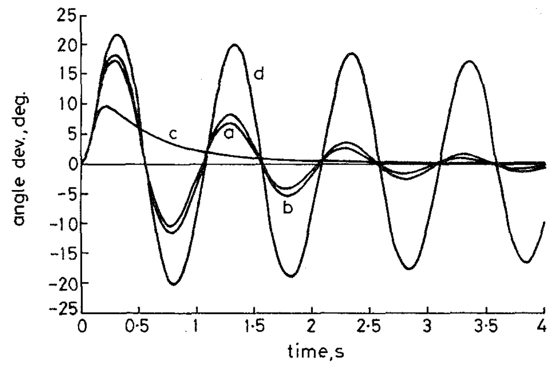

Fig. 5 *Angle deviation for a 50% torque pulse of 0.1 s duration*
(a) state regulator SVC control; (b) output regulator SVC control; (c) proposed optimum SVC control; (d) no control

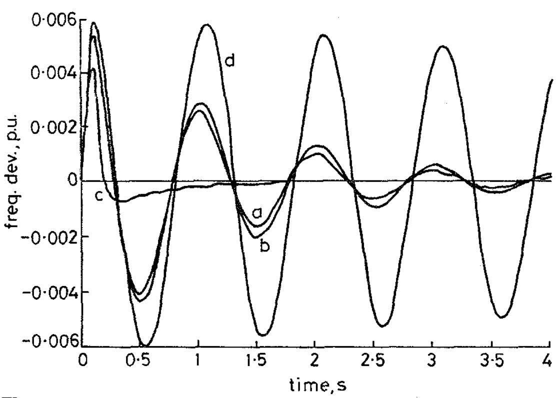

Fig. 6 *Frequency variation corresponding to Fig. 5*
(a) state regulator SVC control; (b) output regulator SVC control; (c) proposed optimum SVC control; (d) no control

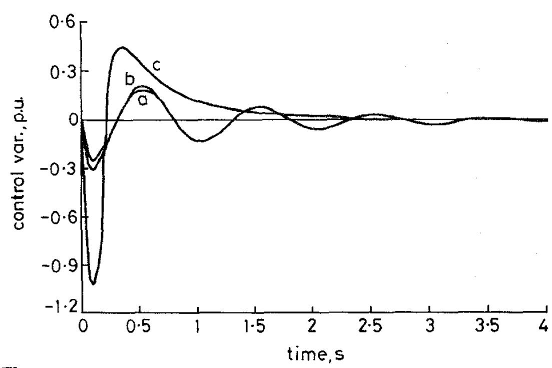

Fig. 7 *Variation of control B in per unit for the 50% disturbance with only SVC stabilising control*
(a) state regulator; (b) output regulator; (c) proposed optimum strategy

Figs. 5 and 6 show the variations of rotor angle and angular frequency deviation of generator ($\Delta\omega$) respectively, following a 50% torque pulse on the generator shaft for a duration of 0.1s with various SVC control stategies. Curves a– d represent the response with state regulator control, output regulator control, proposed optimum control, and no control cases, respectively. While all the three strategies stabilise the system effectively, the proposed feedback strategy is the best as can be observed from the figures. Fig. 7 shows the variation of susceptance B of the SVC in per unit values as is demanded by the various strategies. The SVC supplies capacitive vars at the early part of the transients and then switches to the inductive mode. While several switchings are required by the state regulator and output regulator strategies, there is only one switching with the proposed optimum controller.

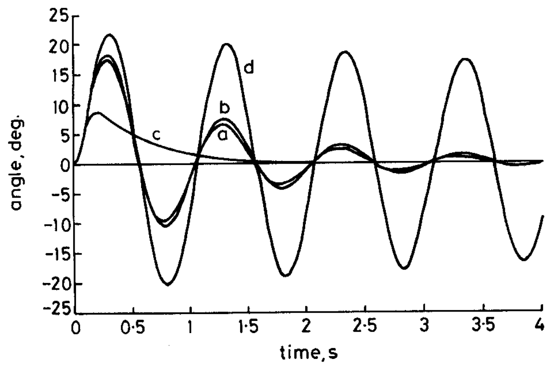

Fig. 8 *Angle variation with combination of SVC and excitation controls for the 50% torque pulse disturbance*
(a) state regulator; (b) output regulator; (c) proposed optimum strategy; (d) no control

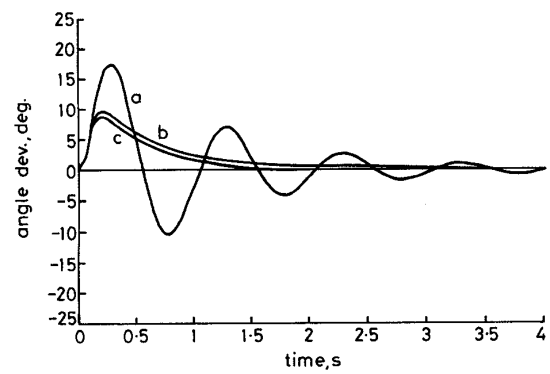

Fig. 9 *Angle time variation for the torque pulse disturbance*
(a) state regulator with SVC only; (b) proposed time optimal control with SVC alone; (c) proposed optimal control through SVC and exciter for the 50% torque pulse

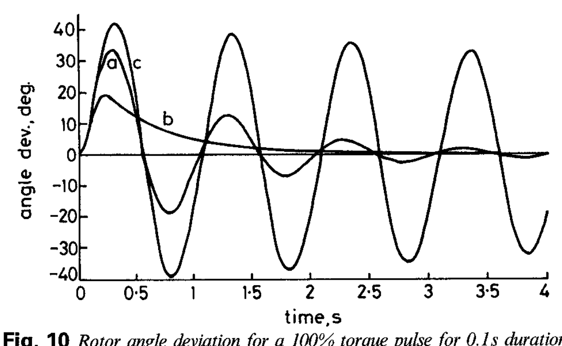

Fig. 10 *Rotor angle deviation for a 100% torque pulse for 0.1s duration with combination of excitation and static VAr control*
(a) state regulator control; (b) proposed optimum feedback control; (c) no control

Fig. 8 shows a comparison of the responses when both SVC and exciter controls are used. Curves a, b, c indicate the responses with state regulator, output regulator, and the proposed minimum time-based controls, respectively. Fig. 9 compares the response with SVC alone with the coordinated SVC and excitation controls applied simultaneously. The response from the state regulator scheme is shown as a reference.

From Figs. 8 and 9 it is apparent that the excitation control on the remote generator is not that effective in providing system damping. Most of the damping is provided by the SVC control. This has been observed with all the three control strategies – the state regulator, the output regulator and the minimum time strategies.

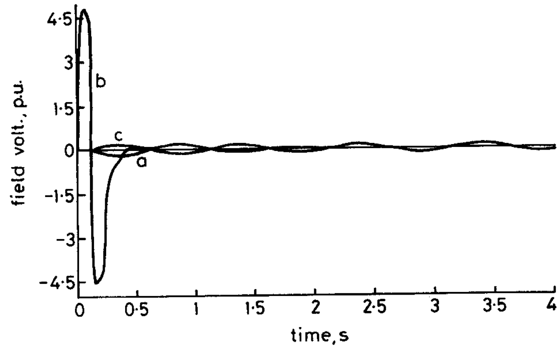

Fig. 11 *The variation of generator field voltage corresponding to the disturbance in Fig. 10*
(a) state regulator control; (b) proposed optimum feedback control; (c) no control

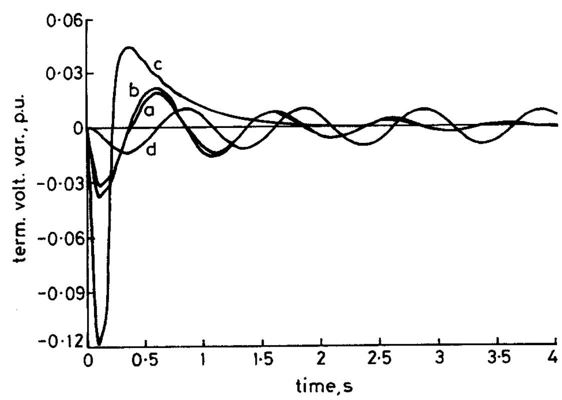

Fig 12 *Terminal voltage variation of generator for the disturbance condition of Fig. 10*

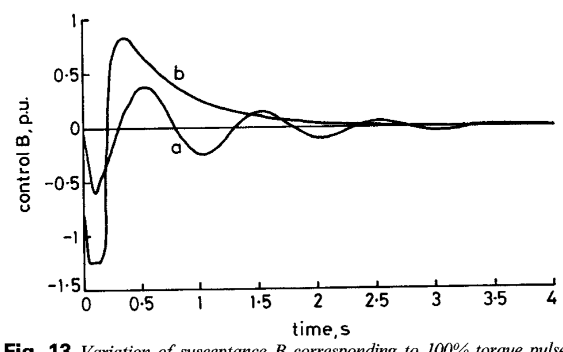

Fig. 13 *Variation of susceptance B corresponding to 100% torque pulse disturbance of Fig. 10*
(a) state regulator strategy; (b) proposed optimum feedback strategy

Figs. 10–13 show the response of the system with a relatively large disturbance of a 100% torque pulse on the generator shaft. While the transient swings generally are of the same nature as the previous disturbance condition, the magnitudes are larger. The proposed controls are equally effective in this larger disturbance case also. Terminal voltage characteristics in Fig. 12 show a relatively large change for a very short duration when the SVC control B is driven to its lower limit.

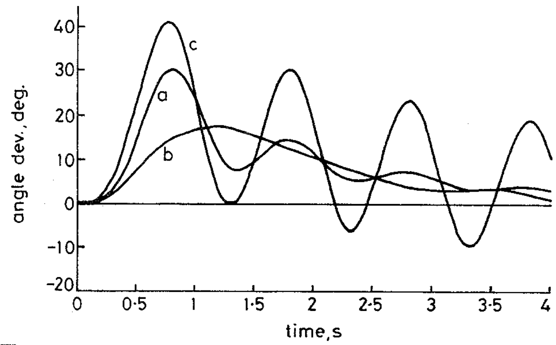

Fig. 14 *Rotor angle variation for a 100% change in reference terminal voltage in the regulator/exciter system for a duration of 0.5s*
The responses are with combination of excitation and SVC control, with (a) the state regulator strategy; (b) proposed optimum strategy; (c) no control

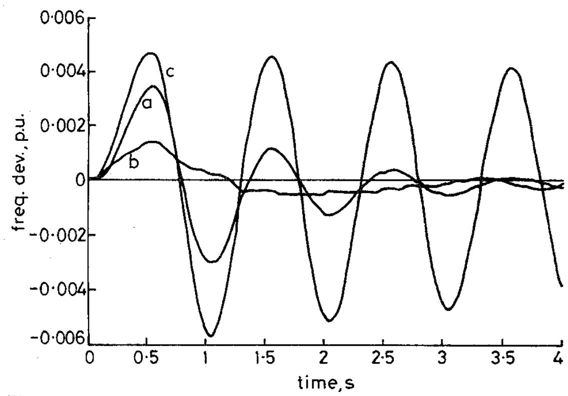

Fig. 15 *Frequency variation characteristics corresponding to Fig. 14*
(a) state regulator strategy; (b) proposed optimum strategy; (c) no control

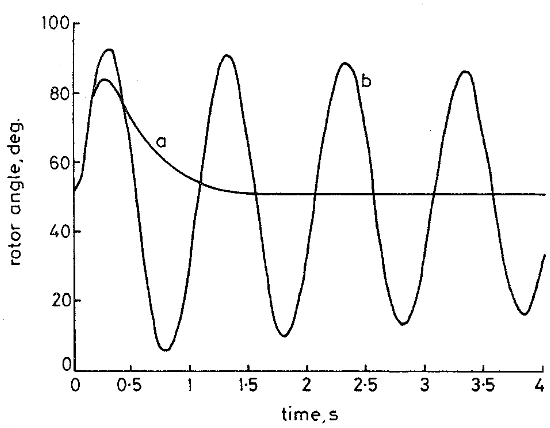

Fig. 16 *Rotor angle variations for a 3-phase fault on the generator terminal cleared in 0.1s*
(a) proposed optimum SVC and excitation control; (b) no control

Figs. 14 and 15 show the generator rotor angle and angular frequency variations following a loss of reference voltage for a duration of 0.5s. The response in the absence of extra stabilising control is totally oscillatory. A combined excitation and static VAr control proposed is able to capture the swings of the machine very quickly (curve b). The frequency variation becomes negligibly small after about 1s and the angle returns to the steady value slowly, virtually without any oscillation.

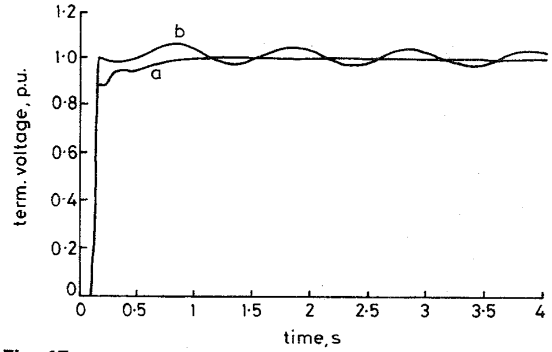

Fig. 17 *Terminal voltage variation of the generator corresponding to the fault condition of Fig. 16*
(a) proposed optimum SVC and exciter control; (b) no control

Figs. 16 and 17 show the variation of rotor angle and terminal voltage of the generator when a three-phase fault is applied to the generator terminal, cleared after 0.1s. The responses are shown with the proposed SVC and exciter control against the uncontrolled case. The response recorded clearly shows that the proposed controller can effectively damp out very large oscillations with a fairly good terminal voltage characteristics.

5.1 Discussion of results

Comparison of the various control strategies presented shows that the proposed minimum time controller of SVC and excitation is most effective in terms of transient control. This is evidenced in all the case studies. As we have seen, the time-optimum SVC and excitation controls given in eqns. 23 and 27 are of the form

$$u = \pm \operatorname{sgn} \Sigma \tag{32}$$

This means that in order to stabilise the system in minimum time so as to bring the rotor speed and acceleration to zero as quickly as possible, the controls should be driven to the limiting values in a manner determined by Σ. There are two difficulties associated with this 'bang-bang' control structure:

(i) The strategies require very fast controllers.

(ii) There may be large variations of variables which depend directly on controls.

One way of overcoming this is to make the control action proportional to the switching function. Let us rewrite eqns. 24 and 28 as

$$u = K\Sigma \tag{33}$$

where, K and Σ are the respective gains and switching functions associated with the SVC and excitation controls. The optimum strategies eqns. 23 and 27 require K to be very large (ideally infinite), whereas no control action implies $K = 0$. K generally will depend on generator sizes and the available control limits. Suitable values are to be determined by trial and error.

The optimum strategy eqn. 32 has the objective of bringing the electromechanical variables to the origin very quickly. The other variables like the voltages and currents will follow the electromechanical ones. Similar to eqn. 11, the terminal voltage of the generator can be expressed as

$$\Delta v_t = r_{32}\Delta e_q' + r_{31}\Delta\delta + r_{33}\Delta B \tag{34}$$

which depends directly on the SVC control ΔB. Since B is driven to the limiting values by the time-optimum strategy, the terminal voltage variation can be relatively large for a very short duration.

The alternative strategy of proportional control given by eqn. 33 will minimise the sharp variation of terminal voltage. However, a very small value of K will not result in significant improvement in the transients. The values of K for the case studies in Figs. 5–17 were chosen to eliminate the transients in less than one second even for a very large disturbance. The terminal voltage for a three-phase fault condition cleared after 0.1s, returned to within 5% of the normal value in about 0.4s, as shown in Fig. 17. However, if faster voltage recovery is desired, the gains can be further reduced. This will result in larger settling times for the transients.

6 Conclusions

Improvement of power system damping through coordinated application of SVC and excitation control has been investigated. An optimal feedback control strategy has been proposed and the results compared with the well known optimum linear state regulator and suboptimum output regulator formulations. For a synchronous generator remotely located from the load centre, it has been observed that most of the damping is provided by SVC control. The coordinated excitation and SVC controls have been observed to be very effective in damping the power system transients.

The control strategies proposed for SVC as well as for excitation are functions of some system states and other measurable variables. This makes on-line implementation of the controllers easy. In this study, a linear system model was chosen in order to evaluate the proposed controller through the standard linear procedures. The proposed control technique can be routinely extended to the nonlinear system model as well as to the multimachine systems as indicated in Section 4.

7 References

1 MEHRAN, A.R., HOGG, B.W., and EL-SAYED, M.L.: 'Coordinated control of synchronous generator excitation and static var compensator', *IEEE Trans. Energy Conv.*, 1992, **7**, pp. 615–622

2 HAMAD, A.E.: 'Application of static var compensators in utility power systems'. IEEE Tutorial Course: Application of Static Var Systems for System Dynamic Performance, 1987, IEEE 87TH 0187-5-PWR, pp. 28–35

3 HAMAD, A.E.: 'Analysis of power system stability enhancement by static var compensators', *IEEE Trans. Power Syst.*, 1986, **1**, (4), pp. 222–227

4 OLIVERIA, S.E.M.: 'Synchronizing and damping torque coefficients and power system steady-state stability as affected by static var compensators', *IEEE Trans. Power Syst.*, 1994, **9**, (1), pp. 109–116

5 ZHOU, E.Z.: 'Application of static var compensators to increase power system damping', *IEEE Trans. Power Syst.*, 1993, **8**, (2), pp. 655–661

6 LARSEN, E.V., and CHOW, J.H.: 'SVC control design concepts for system dynamic performance'. IEEE Tutorial Course: Application of Static Var Systems for Power System Dynamic Performance, 1987, IEEE 87TH 0187-5-PWR, pp. 36–53

7 MARTIN, D.E.: 'SVC consideration for system damping', 1987, pp. 68–71

8 IEE SPECIAL STABILITY CONTROLS WORKING GROUP: 'Static var compensator models for power flow and dynamic performance simulation', *IEEE Trans. Power Syst.*, 1994, **9**, (1), pp. 229–240

9 LERCH, E., POVH, D., and XU, L.: 'Advanced SVC control for damping power system oscillations', *IEEE Trans. Power Syst.*, 1991, **6**, pp. 524–535

10 O'BRIEN, M., and LEDWICH, G.: 'Static reactive power compensator controls for improved system stability', *Proc. IEE C*, 1987, **134**, (1), pp. 38–42

11 MARTINS, N., and LIMA, L.T.G.: 'Determination of suitable locations for power system stabilizers and static var compensators for damping electromechanical oscillations in large scale power systems', *IEEE Trans. Power Syst.*, 1990, **5**, pp. 1455–1469

12 KIRK, D.E.: 'Optimal control theory – An introduction' (Prentice Hall, 1970)

13 KOBAYASHI, H., ICHIYANAGI, K., and FUJITA, Y.: 'Improvement of dynamic stability of parallel AC–DC power system by suboptimal control', *Electr. Eng. Jpn.*, 1978, **98**, pp. 76–83

14 ATHANS, M., and FALB, P.: 'Optimal control' (McGraw Hill, 1967)

15 RAMAR, K., and SRINIVAS, A.: 'Suppression of low frequency oscillations using static var compensator controls', *Electr. Mach. Power Syst.*, 1989, **17**, pp. 109–123

8 Appendices

8.1 Appendix A

Referring to Fig. 1, the voltage at the midpoint of the transmission line can be written as

$$v_m = [v_t + v_o]Z_B^{-1} \tag{35}$$

where,

$$Z_B^{-1} = (2 - BX) + jBR$$

The SVC is represented by a variable susceptance B. Equating the generator current to be the line plus load current, we get

$$i(ZZ_B) = (YZZ_B + Z_B - 1)v_t - v_o \tag{36}$$

Denoting the coefficient of v_t in eqn. 36 to be $C_1 + jC_2$, coefficient of i to be $R_1 + jX_1$, and breaking the currents and voltages into their direct and quadrature axes components, we write

$$\begin{bmatrix} R_1 & -X_1 \\ X_1 & R_1 \end{bmatrix} \begin{bmatrix} i_d \\ i_q \end{bmatrix} = \begin{bmatrix} C_1 & -C_2 \\ C_2 & -C_1 \end{bmatrix} \begin{bmatrix} v_d \\ v_q \end{bmatrix} - v_o \begin{bmatrix} \sin\delta \\ \cos\delta \end{bmatrix} \tag{37}$$

The coefficients in eqn. 7 can be expressed as

$$R_2 = R_1 - C_2 x'_d, \quad X_2 = X_1 + C_1 x_q, \quad X_3 = X_1 + C_1 x'_d,$$
$$R_3 = R_1 - C_2 x_q, \quad Z_e^2 = R_2 R_3 + X_2 X_3,$$
$$Y_d = (C_1 X_2 - C_2 R_3)/Z_e^2, \quad Y_q = (C_1 R_2 + C_2 X_3)/Z_e^2 \tag{38}$$

Further, the voltage at the mid point of the line can be written as

$$v_m = v_t - i_1 Z \tag{39}$$

where,

$$i_1 = i - i_L$$

The currents and voltages can be broken up to their d/q axes components. The power flow at the mid point of the line is

$$P_m = v_{md} i_{1d} + v_{mq} i_{1q} \tag{40}$$

Expressing the line currents in terms of the generator currents and linearising we can arrive at eqn. 11.

When eqn. 37 is solved for the currents i_d and i_q and linearised, it takes the form [15]

$$\begin{aligned} \Delta i_d &= Y_d \Delta e'_q + F_d \Delta\delta + H_d \Delta B \\ \Delta i_q &= Y_q \Delta e'_q + F_q \Delta\delta + H_q \Delta B \end{aligned} \tag{41}$$

These expressions of currents when substituted in the linearised expressions for electrical power output, internal voltage equation, field equation and the electromechanical swing equations , the system dynamics given by eqn. 10 are obtained.

8.2 Appendix B

The system data taken from [15] are (in p.u.): $R = 0.01$, $X = 0.3$, $g = 0.04$, $b = -0.38$, $x'_d = 0.45$, $x_d = 1.7$, $x_q =$

1.25, $H = 4$s, $K_A = 4.0$, $T_A = 0.03$.

The initial values are: $\delta = 52°$, $e_q' = 1.1808$, $v_t = 1.0 \angle 16°$, $P = 0.866$, $Q = 0.392$, $v_0 = 1.0$.

The system matrices are:

$$\mathbf{A} = \begin{bmatrix} 0 & 377 & 0 & 0 \\ -0.1029 & 0 & 0 & -0.1253 \\ 7.21 & 0 & -33.33 & -6.185 \\ -0.1484 & 0 & 0.1587 & -0.373 \end{bmatrix}$$

$$\mathbf{b} = \begin{bmatrix} 0 & 0 \\ 0.03218 & 0 \\ -10.38 & 133.33 \\ 0.05256 & 0 \end{bmatrix}$$

Further,

$$\begin{bmatrix} \Delta v_m \\ \Delta p_m \end{bmatrix} = \begin{bmatrix} -0.031 & 0.1128 & 0.2157 \\ 0.862 & -0.2064 & 0.6248 \end{bmatrix} \begin{bmatrix} \Delta\delta \\ \Delta e_q' \\ \Delta B \end{bmatrix}$$